UNIVERSITY OF AMSTERDAM

UvA-DARE (Digital Academic Repository)

A suit of armor around ADAMTS13

Exploring paths towards resistance against autoantibodies of immune TTP patients

Gomes Graça, N.A.

Publication date
2021

Link to publication

Citation for published version (APA):
Gomes Graça, N. A. (2021). *A suit of armor around ADAMTS13: Exploring paths towards resistance against autoantibodies of immune TTP patients*. [Thesis, externally prepared, Universiteit van Amsterdam].

General rights
It is not permitted to download or to forward/distribute the text or part of it without the consent of the author(s) and/or copyright holder(s), other than for strictly personal, individual use, unless the work is under an open content license (like Creative Commons).

Disclaimer/Complaints regulations
If you believe that digital publication of certain material infringes any of your rights or (privacy) interests, please let the Library know, stating your reasons. In case of a legitimate complaint, the Library will make the material inaccessible and/or remove it from the website. Please Ask the Library: https://uba.uva.nl/en/contact, or a letter to: Library of the University of Amsterdam, Secretariat, P.O. Box 19185, 1000 GD Amsterdam, The Netherlands. You will be contacted as soon as possible.

UvA-DARE is a service provided by the library of the University of Amsterdam (https://dare.uva.nl)

Download date:17 Nov 2026

6

Chapter 6

Modelling-assisted identification of CUB1/2 domain residues involved in maintaining ADAMTS13 in a closed conformation

Bogac Ercig*, Tom Arfman*, **Nuno A. G. Graca***, Kanin Wichapong, Elien Roose, Paul Kaijen, Chris Reutelingsperger, Karen Vanhoorelbeke, Gerry A.F. Nicolaes, Jan Voorberg

These authors contributed equally

Manuscript in preparation

Abstract

Most patients with immune-mediated thrombotic thrombocytopenic purpura (iTTP) develop autoantibodies targeting a cryptic epitope in the spacer domain of ADAMTS13. The spacer domain epitope is composed of residues R568, F592, R660, Y661 and Y665 is inaccessible when ADAMTS13 is in a closed conformation. A recent study has shown that ADAMTS13 circulates in open conformation during the acute phase of iTTP, suggesting that conformational changes of ADAMTS13 contribute to the pathogenesis of iTTP. We employed structural bioinformatics to build a 3D model of the closed conformation of ADAMTS13 to identify CUB domain residues which interact with the spacer domain thereby keeping ADAMTS13 in a closed conformation. Our model predicted several candidate CUB1 and CUB2 domain residues that could potentially interact with the spacer domain. These CUB domain residues were selected for *in vitro* mutagenesis study and we used a previously established ELISA-based assay which utilizes the CUB domain specific monoclonal antibody 17G2 to determine whether these variants are present in an "open" or "closed" conformation. ADAMTS13 variants D1240A, L1243A, R1247E, P1333A and R1336E variants were constitutively present in an open conformation suggesting that these residues contribute to spacer-CUB1/2 domain interactions. Proteolytic activity of D1240A, L1243A, L1248A, P1333A and R1336E towards VWF multimers was more efficient when compared to wild type ADAMTS13. Overall, our structural bioinformatics guided approach has uncovered several CUB1/2 domain residues which are critical for maintaining ADAMTS13 in a closed conformation.

Introduction

Adhesion of platelets to sites of vascular injury is critically dependent on the multimer size of von Willebrand Factor (VWF) (1). **A D**isintegrin **A**nd **M**etalloprotease with **T**hrombo**S**pondin type-1 repeats, number **13** (ADAMTS13) regulates multimer-size of VWF through by cleavage of a scissile bond between Y1605 and M1606 in the unfolded A2 domain (2). The physiological relevance of ADAMTS13 is illustrated by the thrombotic complications in patients with thrombotic thrombocytopenic purpura (TTP) who lack functional ADAMTS13 (3). In the majority of patients, TTP develops due to the presence of anti-ADAMTS13 autoantibodies which result in proteolytic inhibition (4) or faster clearance (5) of ADAMTS13. This subtype of TTP is called immune-mediated TTP (iTTP) (3). Most of the anti-ADAMTS13 autoantibodies target the spacer domain which is known to be an interaction hub for ADAMTS13 (6, 7) as it provides an exosite for VWF (8). Moreover the carboxy-terminal CUB domains bind to spacer domain thereby maintaining ADAMTS13 in a closed conformation (Figure 1A) (9, 10).

C-terminal CUB domains (complement components C1r and C1s, sea urchin protein Uegf, and bone morphogenetic protein-1) are the main feature that sets ADAMTS13 apart from the other members of the ADAMTS family of proteins (11). CUB domains mediate protein-protein interactions and are mostly part of extracellular or plasma membrane associated proteins (12). CUB domains have been implicated in many physiological processes such as; complement activation (13), tissue repair (14), cell signaling (15), tumor suppression (16), inflammation (17) and hemostasis (6). CUB domains are auxiliary structures to catalytic domains as in complement proteases, in which they are responsible of dimer formation or binding to collagen-like regions of C1q (18). CUB domains as present in cubilin are responsible for intestinal uptake of intrinsic factor and vitamin B_{12} (19). Usually, CUB domains have 4 cysteines residues which form 2 disulfide bonds on the upper loops of a beta-sandwich structure (12). However, the ADAMTS13 CUB1 domain has 5 cysteine residues and CUB2 has 2 cysteine residues (20). The additional CUB1 domain cysteine residue C1275 is not conserved between different species (6, 21). Interestingly, three independent studies have shown that ADAMTS13 CUB domain cysteine residues are found at least in part as free thiols (22–24), in contrast to other known CUB domains in which cysteines form disulfide bonds. Also, a subset of CUB domains have functionally conserved negatively charged residues which are responsible for binding a Ca^{2+} ion for ligand recognition (12). However this feature is not present in ADAMTS13 (6). ADAMTS13 CUB domains have two known functions: 1) ADAMTS13 C-terminal domains form a hairpin-like structure and CUB domains bind to spacer domain to regulate substrate specificity of ADAMTS13 (closed conformation) (9, 25), 2) in circulation, ADAMTS13 CUB domains bind to VWF-D4CK domains (26). Binding of ADAMTS13 to the VWF-

D4CK domains leads to conformational "opening" of ADAMTS13 in preparation for VWF proteolysis (9). Binding of CUB domains to VWF-D4CK abolishes spacer-CUB domain interactions which allow for binding of exosite within the spacer domain to the unfolded A2 domain (27, 28). Next, exosites on cysteine-rich and disintegrin-like domain bind to VWF to position the scissile bond in the VWF A2 domain for proteolysis by ADAMTS13 (29). Binding of disintegrin-like domain exosite allosterically activates metalloprotease domain which increases the turnover number (k_{cat}), resulting in higher proteolytic activity against VWF (30, 31).

Several structural studies has shown that ADAMTS13 may adopt different conformations such as open, closed or intermediates (9, 25, 32, 33). Importantly, it was recently shown that ADAMTS13 circulates in an "open" conformation during the acute phase in patients with iTTP whereas it circulates in a closed conformation in iTTP patients in remission and healthy individuals (34). Follow-up studies revealed that patient-derived antibodies are capable of converting ADAMTS13 from a closed to an open conformation (35). These findings position conformational changes of ADAMTS13 as a clinically relevant biomarker of iTTP which occurs as an early event that precedes the appearance of detectable titers of anti-ADAMTS13 autoantibodies (35). Despite its physiological and pathophysiological importance we currently do not know which CUB domains residues are responsible for maintaining ADAMTS13 in a closed conformation.

Here we investigate the CUB-domain residues that bind the spacer domain using a molecular modelling approach. Based on *in silico* binding free energy (BFE) calculations, single/multiple alanine variants of target residues were created and characterized to investigate their effect on ADAMTS13 conformation and activity.

Material and Methods

Chemicals, reagents and materials

Subcloning Efficiency™ DH5α competent cells, Fastdigest Enzymes MreI and XhoI, ExpiCHO cell line and ExpiFectamineCHO transfection kit (Thermo Scientific), Amicon Ultra-15 centrifugal filter with 30 kDa cutoff (Merck), bovine serum albumin fraction V (BSA; Serva, Germany), tetramethylbenzidine (TMB; Thermo Scientific), streptavidin-horseradish peroxidase (HRP) and anti-V5-HRP (Thermo Scientific), FRETS-VWF73 Substrate (Peptides International), SeaKem HGT agarose (Lonza, Belgium), iBlot (Thermo Scientific), rabbit anti-human VWF-HRP polyclonal antibody (Dako), DAB substrate kit (Vector Laboratories, USA) were used for this study. ADAMTS13 antibodies 3H9, 17G2, 19H4, 1C4, 3E4 and 6A6 have been described previously (31, 32, 34)

Molecular modeling of ADAMTS13 Closed conformation

ADAMTS13 CUB domains structures were built by using homology modeling in YASARA Structure (36) with the following templates (Protein Data Bank (PDB) ID: 2QQL, 3KQ4, 4GZ9). Homology models were refined with a short molecular dynamics simulation (500ps) in YASARA to correct bond length and geometry (Figure 1B) (36). The possible complexes between cysteine-rich/spacer (PDB ID: 3GHM) and CUB domains were generated using HADDOCK protein-protein docking (37). The docking process is driven by ambiguous interaction restraints (AIRs) in which spacer domain R568/F592/R660/Y661/Y665 were selected as active residues and the glycan containing sites (38); N579/N614/N667 were selected as negative residues. In 3D CUB models, we employed CPORT (39) to predict which residues are the active interface residues to drive the docking process and the glycan sites (38); N1235/S1312/N1354 were selected as negative residues (Figure 1C). All docking poses generated by HADDOCK were further duplicated into a second set, in which gain-of function (GoF) ADAMTS13 mutations (R568K/F592Y/R660K/Y661F/Y665F) (40) were introduced using PyMOL 1.8.2.1 (The PyMOL Molecular Graphics System, Version 1.8.2.1 Schrödinger, LLC). Both wild type (WT)- and GoF-spacer-CUB complexes were prepared for subsequent molecular dynamics (MD) simulations using AMBER16 and AmberTools16, assigning the FF14SB forcefield for 100ns simulation time (Figure 1D) (41). MMPBSA.py (42) was employed to calculate the BFE between the spacer domain and the CUB domains. In this study, the BFE difference between WT- and GoF-ADAMTS13 against CUB domains was used as a selection criterion. In agreement with data reported in the literature (10), CUB domains bind to WT-spacer, whereas they do not bind to GoF-spacer (40). After each interval of 10 ns MD simulation, each WT-pose with a lower BFE compared to its GoF-pose was kept, otherwise was discarded. The BFE decomposition per residue was calculated after each 10 ns interval of the MD simulation, in order to obtain a better understanding of the interactions at atomic level which provided a further insight on exploring which residues of CUB domains are mediating the binding to spacer domain (Figure 1E). Several residues from both CUB1 and CUB2 domains were selected for *in vitro* mutagenesis study based on the modeling.

Plasmid preparation and protein expression

Mutant DNAs flanked by MreI and XhoI restriction sites were ordered in pUC17 vectors (Baseclear, the Netherlands). After upscaling, these constructs were digested by MreI and XhoI. Subsequently the mutant gene fragments were used to replace the CUB domain sequence in WT-ADAMTS13 pcDNA3.1+ with a C-terminal V5 and His-tag. Mutant ADAMTS13 constructs were sequenced, amplified and purified. ExpiCHO cell lines were used as transient expression system for WT-ADAMTS13 and CUB domain variants. Transfections were carried out according to manufacturer's guidelines. All variants were produced in 6-well plates in 2.5 ml volume. CUB variants with low

expression levels, were produced in 25 ml and concentrated using Amicon Ultra-15 centrifugal filters; 10 mM benzamidine was added to culture media after collection.

Concentration determination of ADAMTS13 CUB domain variants

ADAMTS13 concentration in cultured media was detected as previously explained (7, 43). Briefly, 96-well plates were coated with 3H9 (5 µg/ml), blocked with 2% BSA-PBS (w/v). WT-ADAMTS13 and CUB domain variants were incubated for capturing. Next, captured variants were targeted with 17G2 and 19H4 (both biotinylated; 1.5 µg/ml, each), later detected with streptavidin coupled with horseradish peroxidase (diluted in 1:10000). Colorimetric development was performed with TMB and reaction was stopped with 1M H_2SO_4. Absorbance was measured at 450 nm using a plate reader. A normal human plasma (NHP) pool was used as calibrator and set at 1 µg/ml. All variants were also detected in western blot with anti-V5-HRP antibody (1:20000).

FRETS-VWF73 activity assay

FRETS-VWF73 assay to measure the activity of each variant was carried out as previously explained (7). Diluted culture media containing the WT-, MDTCS-ADAMTS and CUB variants at a concentration of 1.05 nM (0.2 µg/ml) were used for the FRETS-VWF73 assay. ADAMTS13 was first diluted in an activity buffer composed of 20 mM HEPES, 20 mM Bis-Tris, 20 mM Tris-HCl, 25 mM $CaCl_2$ (pH 6.0) supplemented with 0.005% Tween-20 to 2.1 nM in a 100 µl volume. Then, the reaction was started by adding FRETS-VWF73 substrate (100 µl, 4 µM), diluting further ADAMTS13 to 1.05 nM. In parallel, a calibration curve was generated in a similar manner using the WT-ADAMTS13 diluted in a concentration range of 0.13125–2.10 nM. The activity levels of the ADAMTS13 variants were calculated and compared to that of WT-ADAMTS13 with final concentration of 1.05 nM, which was set at 100%.

VWF multimer activity assay

To measure the ability of different ADAMTS13 variants to process VWF multimers 0.2 µg of each ADAMTS13 variant was incubated for 30 mins at 37°C in an activation buffer composed of 20 mM Bis-Tris, 20 mM Tris-HCl, 20 mM HEPES, 25 mM $CaCl_2$ (pH 7.5), 0.005% Tween 20 and supplemented with 2% BSA (final concentration ADAMTS13 3.8 nM). In parallel, recombinant VWF was incubated with 3 M urea for 30 min at 37°C at a final concentration of 40 nM. Denatured recombinant VWF multimers were then added to the ADAMTS13 containing mixture at a 1 to 1 ratio (final ADAMTS13 concentration 1.9 nM; final concentration VWF 40 nM). Samples were collected and quenched with 4x SDS-PAGE loading buffer containing 25 mM EDTA at 0 and 30 minutes and 24 hours to assess the ability of the different ADAMTS13 variants to process VWF. Samples were collected and quenched with 4x SDS PAGE loading buffer at 0 and 30 minutes and 24 hours to assess the ability of the

different ADAMTS13 variants to process VWF. All collected samples were analyzed by 2% agarose gel electrophoresis. Next, proteins were transferred to a PVDF membrane using iBlot (Thermo Scientific, USA) for 10 minutes at 20V. Membranes were air-dried for 30 minutes, activated with methanol and incubated with anti-VWF-HRP antibody (1:2000). VWF multimers were visualized directly on PVDF membrane using DAB stain (Vector Laboratories, USA).

Open/closed conformation ELISA

WT-ADAMTS13 and all CUB domain variants were screened for conformational phenotype as previously explained (34). All samples (dilutions from 0.4 to 0.1 ug/ml) were treated with both 17G2 (2.5µg/ml) to open ADAMTS13 and variants up as a positive control or with 1% BSA-PBS to keep ADAMTS13 and variants in their native conformation. 96 well-plate was coated with 1C4 (5µg/ml), an antibody which captures ADAMTS13 from a cryptic epitope in spacer domain. Captured ADAMTS13 was detected with anti-V5-HRP antibody (1:2500) and colorimetric development was carried out as explained above. Induction of open conformation by means of the 17G2 antibody increases capturing of ADAMTS13 by 1C4 which leads to a higher OD output. This OD increase is not expected for mutants that are already in open conformation. WT-ADAMTS13 known to be in closed conformation was used as a control.

Results

3D model of ADAMTS13 Closed conformation

A likely binding mode between ADAMTS13 spacer domain and its CUB domains was found using our modeling strategy (Figure 1). We compared our BFE calculations with previously measured K_D values from literature (10). We computed the BFE between WT-spacer domain and CUB domains to be -62±11 kcal/mol and -39±12 kcal/mol for GoF-spacer domain and CUB domains. Since, only WT-spacer domain can bind to CUB domains (10), we obtained a lower BFE (higher affinity) for WT-complex. Even though, CUB domains do not bind to GoF-spacer domain, in our simulations we were still able to compute a BFE between GoF-spacer and CUB domains due to the binding of charged and unstructured C-terminal tail of the CUB2 domain. We computed a higher BFE (-13 kcal/mol; lower affinity) for spacer-CUB1 interactions which also had a higher K_D (135±10 nM) than CUB2 (BFE: -50±8 nM, K_D: 87±9 kcal/mol). As previously shown, CUB1 domain binds to spacer domain and cause inhibitory effects on VWF proteolysis (10). Our model shows that CUB1 domain is binding and causing a steric hindrance to exosite residues (R568/F592/R660/Y661/Y665) on spacer domain which can explain these inhibitory effects. Based on careful investigation of the complex and BFE decomposition per residue, we have identified several residues from both

CUB1 and CUB2 domains which were predicted to be the mediators of spacer-CUB domain interaction during closed conformation. These residues are D1240, M1241, L1243, R1247, L1248 from CUB1 domain, P1333, R1336, E1382, S1383 and S1384 from CUB2 domains (Figure 2). These residues were selected for an *in vitro* alanine scanning, and the resulting variants were screened for their impact in CUB1/2 spacer domain interactions. Additionally, we prepared a set of charge inversion mutants such as D1240R, R1247E, R1336E, E1382R.

CUB domain variants express at different levels

ADAMTS13 variants were transiently expressed in ExpiCHO cells (Table 1). Most CUB domain variants were expressed or secreted at lower concentrations than WT-ADAMTS13. Any variant that contains a D1240A substitution in CUB1 domain, a R1336E and combination of multiple substitutions in CUB2 domain resulted in lower expression or secretion levels and they were concentrated to be able to reach minimum required concentrations for the assays (Table 1). CUB1 domain variants M1241A, L1243A, R1247A, R1247E, L1248A were expressed at similar levels as WT-ADAMTS13. CUB2 domain variants P1333A, R1336A, E1382A, E1382R, S1383A, S1384A were also expressed at similar levels as WT-ADAMTS13.

Activity level of CUB variants depend on their conformation

In open conformation, CUB domains no longer display autoinhibitory effects on spacer domain, which eventually results in conformational activation of metalloprotease domain (30, 31). Catalytic activity of ADAMTS13 significantly increases following the activation of metalloprotease domain. For this reason, we measured the activity of each CUB variant to check whether the introduced substitutions affect the proteolytical activity towards FRETS-VWF73 and VWF multimer substrates. In FRETS-VWF73, we observed increased activity for L1248A and L1243-48A in CUB1 (Figure 3A). We were unable to assess the ability of D1240A, D1240A-M1241A, D1240A-M1241A-R1247A, 5X-CUB1, R1336E, R1336A-S1383A-S1384A and 5X-CUB2 due to interference of the concentrated culture medium in the FRETS-VWF73 activity assay. The activity of CUB1 domain variants M1241A, R1247A, L1243A, R1247E and L1248A was similar to that of WT-ADAMTS13 (Figure 3A). The activity of L1248A was 135% and L1243A-L1248A was 180% when compared to WT-ADAMTS13 suggesting that these variants are more efficient in converting FRETS-VWF73. The CUB2 domain variants P1333A, R1336A, E1382A, E1382R, S1383A and S1384A has similar activity as WT-ADAMTS13 (Figure 3A). Next, we analyzed the ability of the generated ADAMTS13 variants to process VWF multimers. VWF multimer assay provided additional input on concentrated material since the activity readout does not depend on fluorescence. In this assay, CUB1 domain variants were shown to be able to efficiently process VWF multimers with the exception of the M1241A variant (Figure 3B). Inspection of the multimeric patterns suggested that variants containing D1240A substitutions,

L1243A, L1248A, L1243-48A, R1336E, and multiple CUB2 domain substitution variants were more active when compared to WT-ADAMTS13. Surprisingly, M1241A was unable to efficiently process VWF multimers (Figure 3B) whereas processing of FRETS-VWF73 substrate was not impaired (Figure 3A). Apparently M1241 is needed for efficient processing of VWF multimers and we speculate that this residue provides a potential docking site for VWF in the CUB1 domain of ADAMTS13. The CUB2 domain variants included in this study were all capable of processing VWF multimers. The proteolytic activities of all variants relative to WT-ADAMTS13 as measured by both FRETS-VWF73 and VWF multimer assays are presented in Table 2.

Open/closed conformation screening for CUB domain variants

ADAMTS13 variants were tested in open/closed conformation ELISA which utilizes the anti-CUB1 monoclonal antibody 17G2 to induce accessibility of monoclonal antibody 1C4 to exosite-3 in the spacer domain. First, we assessed whether all variants were capable of binding to 17G2. All variants with the exception of variants containing D1240A were capable of binding 17G2 (Figure 4A). This observation suggests that D1240 is a crucial part of the epitope of 17G2. All variants including D1240A containing mutants were still able to bind the anti-TSP8 domain antibody 19H4 (Figure 4B). Our controls in this assay were WT-ADAMTS13 for closed conformation and MDTCS for open conformation. Measured OD values represent the availability of 1C4 epitope (anti-spacer) for each variant without 17G2 incubation (native conformation) was compared to with 17G2 incubation (forced open conformation) to observe the native conformational phenotype of each variant. Among all CUB1 domain variants L1243A and R1247E from CUB1 domain were found to be in open conformation (Figure 5). Also the double variant L1243A-L1248A was present in an open conformation. The conformation of D1240A containing variants could not be assessed due to lack of reactivity with 17G2. However, D1240A containing variants were captured by 1C4 at the same level as other ADAMTS13 CUB variants when they were treated with 17G2. This observation indicates that D1240A containing variants adopt an open conformation. P1333A and R1336E from CUB2 domain were found to be in an open conformation (Figure 5). R1336A, E1382A, E1382R, S1383A and S1384A were found to be in a closed conformation with 17G2 (Figure 5). However, variants containing R1336A-S1383A-S1384A and 5x-CUB2 were present in an open conformation (Figure 5). The conformational status of all CUB domain variants is summarized in Table 2.

Discussion

In this study, structural bioinformatics methods were successfully employed to generate a model for ADAMTS13 in a closed conformation. The resulting model was

used to unravel spacer-CUB domain interactions that contribute to conformational control of ADAMTS13. The plasma ADAMTS13 circulates in a closed conformation that is maintained by spacer-CUB domain interactions (34). Upon binding to its substrate VWF, ADAMTS13 converts from a closed, inactive configuration to an open, enzymatically active conformation (9, 32, 44). An open conformation has also emerged as a promising biomarker since elevated levels of "open" ADAMTS13 circulate in the plasma of patients with iTTP during the acute phase (34, 35, 45). It has been well-established that residues present in exosite-3 of the spacer domain are crucial for maintaining ADAMTS13 in a closed conformation (9, 32, 44). As yet we do not know which CUB domain residues contribute to its binding to the spacer domain. Identification of these CUB domain residues will improve our understanding on regulation of ADAMTS13 proteolytic activity and may provide further insights into conformational changes linked to the onset of iTTP.

Up to this date, there are no experimentally determined 3D structures for the closed conformation of ADAMTS13. In this study, we employed a structural bioinformatics pipeline which allowed us to predict amino acid residues in the CUB1 and CUB2 domains that are potentially involved in binding to the spacer domain. *In vitro* alanine scanning suggested that D1240, L1243 and P1333 interact with the spacer domain (Figure 5). Further analysis of charge inverting mutations revealed that also R1247 and R1336 might contribute to spacer domain (Figure 5). The observed phenotype for the D1240A variant is interesting; variants containing this amino acid substitution were expressed at very low levels (Table 1). Due to the low levels of release we were unable to assess whether these variants can convert the FRETS-VWF73 substrate (data not shown). Variants containing the D1240A substitution were however capable of processing VWF multimers with a somewhat higher efficiency when compared to WT-ADAMTS13 (Figure 3B). We also show in this study that the D1240A variant does not bind to 17G2 (Figure 4A). Monoclonal antibody 17G2 has been shown to induce an "open" conformation of ADAMTS13 (34, 35). We propose that ADAMTS13 has the ability to shuttle between a closed and open conformation; under quiescent conditions ADAMTS13 appears to be primarily present in a closed conformation. Upon binding of the carboxy-terminal CUB1/2 domains to VWF, this equilibrium shifts from a closed to an open conformation. Similarly, binding of 17G2 result in a shift in equilibrium from a closed to an open conformation allowing for more extensive binding of the anti-spacer domain antibody 1C4. Our data identify D1240 as a crucial residue for binding of 17G2. Our modelling studies predict that D1240 interacts with R660 in exosite-3 of the spacer domain. Binding of 17G2 to an antigen surface containing D1240 is expected to disrupt this interaction thereby "converting" ADAMTS13 into an "open" conformation. Mechanistically, breaking the interactions between spacer and CUB domains is expected to cause a pre-activation of the latent metalloprotease domain, which is reflected as increased proteolytic activity against VWF (31). We observed

that the proteolytic activity of the open conformation ADAMTS13 variants towards VWF multimers was similar or slightly increased when compared to WT-ADAMTS13. The proteolytic activity of the L1243A-L1248A variant was significantly higher in the FRETS-VWF73 assay whereas also its ability to process VWF multimers appears to be increased (Figure 3). Interestingly, the M1241A variant was not able to process VWF multimers whereas it retained its ability to process the small FRETS-VWF73 substrate (Figure 3). We speculate that M1241 provides a contact-residues in the CUB1 domain needed for binding to the carboxy-terminal VWF D4-CK domain (10). Apart from the carboxy-terminal CUB domains TSP-8 has been proposed to be crucial for binding of ADAMTS13 to VWF as well as for maintaining ADAMTS13 in a closed conformation (10). We did not include TSP-8 in our modelling studies and therefore we cannot exclude that residues in TSP8 might also contribute to maintaining ADAMTS13 in a closed conformation.

In this study, we were able to build a 3D model which is well in agreement with findings recorded in the literature. The previously measured K_D values between spacer and each individual CUB domains (10) showed a similar trend when compared to our computed BFE. We also have observed that our model is sensitive to pH changes; at pH 6 WT-ADAMTS13 was primarily present in an open conformation when compared to pH 7.4 (9, 33). When we simulated our 3D model on different pH levels, we have computed a much higher BFE (lower affinity) at pH 6 than pH 7.4 (data not shown). Additionally, our model claimed that the closed conformation driving residues of CUB domains are located in the upper loops of beta-sandwich structure, which were previously described as immunogenic peptides of iTTP patients, such as in CUB1 residues between 1239-1253 (46) and in CUB2 residues between 1321-1340 (47). This observation might suggest that these T-cell epitopes are only available when ADAMTS13 adopts an open conformation following its entry into low pH endocytic compartments (48, 49). Considering the relevance of open conformation as a biomarker of subclinical TTP, conformational changes might be needed to access cryptic T-cell epitopes, resulting in more efficient CD4+ T-cell response, as observed in other autoimmune diseases (50).

ADAMTS13 is a plasma glycoprotein which carries several N and O-glycans; the spacer domain contains three different N-glycans whereas the CUB domains contain two N-glycans and one O-glycan (38). In our docking process, we considered residues to which these glycans were attached as inactive AIRs. We have not included the N-linked and O-linked glycans present in the spacer and CUB domains in our studies. This provides one of the potential limitations of our model. In a previous study (51), removal of CUB domain N-glycans attached to N1235 and N1354 by N to Q mutations shifts ADAMTS13 to open conformation. Similarly, N-glycans attached to the spacer domain at N579, N614 and N667 may also affect its interaction with the CUB domains. Whether this reflects a direct role for N-glycans in controlling ADAMTS13 conformation requires further study; removal of N-glycans may simply induce loss of

structural stability thereby inducing conformational changes (52). Another potential limitation of our study concerns the impact of mutations on ADAMTS13 secretion. Impaired secretion has been observed for many variants containing congenital TTP causing ADAMTS13 mutations (53). ADAMTS13 CUB domains affect protein secretion by contributing to the apical sorting of the enzyme. This is illustrated by a naturally occurring congenital ADAMTS13 mutation (4143-4144insA) which caused an early stop in CUB2 domain and significantly reduced ADAMTS13 secretion (54). In our study, ADAMTS13 variants containing a D1240A substitution, R1336E as well as the variant containing multiple CUB2 domain mutations were causing secretion defects.

Our model was able to identify several CUB domain residues which contribute to closed conformation of ADAMTS13. Further validation of the model obtained employing relatively low-throughput structural methods such as, hydrogen-deuterium mass spectrometry, X-ray crystallography or cryo-electron microscopy can be used to identify additional determinants for spacer CUB domain interactions. This knowledge will help us to better understand the conformational regulation of the ADAMTS13-VWF axis. Based on the results of these studies it might be feasible to generate CUB domain variants that do not open upon binding of pathogenic antibodies of iTTP patients but can be selectively converted into an active conformation by VWF. Such improved ADAMTS13 variants could be potentially useful for the treatment of patients with iTTP.

References

1. Leebeek, F. W. G., and Eikenboom, J. C. J. (2016) Von Willebrand's disease. *N. Engl. J. Med.* **375**, 2067–2080
2. Furlan, M., Robles, R., Solenthaler, M., and Lämmle, B. (1998) Acquired deficiency of von Willebrand factor-cleaving protease in a patient with thrombotic thrombocytopenic purpura. *Blood*. **91**, 2839–46
3. Kremer Hovinga, J. A., Coppo, P., Lämmle, B., Moake, J. L., Miyata, T., and Vanhoorelbeke, K. (2017) Thrombotic thrombocytopenic purpura. *Nat. Rev. Dis. Prim.* **3**, 1–17
4. Pos, W., Luken, B. M., Kremer Hovinga, J. A., Turenhout, E. A. M., Scheiflinger, F., Dong, J. F., Fijnheer, R., and Voorberg, J. (2009) VH1-69 germline encoded antibodies directed towards ADAMTS13 in patients with acquired thrombotic thrombocytopenic purpura. *J. Thromb. Haemost.* **7**, 421–428
5. Thomas, M. R., de Groot, R., Scully, M. A., and Crawley, J. T. B. (2015) Pathogenicity of Anti-ADAMTS13 Autoantibodies in Acquired Thrombotic Thrombocytopenic Purpura. *EBioMedicine*. **2**, 942–952
6. Ercig, B., Wichapong, K., Reutelingsperger, C. P. M., Vanhoorelbeke, K., Voorberg, J., and Nicolaes, G. A. F. (2018) Insights into 3D Structure of ADAMTS13 : A Stepping Stone towards Novel Therapeutic Treatment of Thrombotic Thrombocytopenic Purpura. *Thromb. Haemost.* **118**, 28–41
7. Graca N A.G., Ercig, B., Velasquez Pereira, L. C., Kangro, K., Kaijen, P., Nicolaes, G. A. F., Veyradier, A., Coppo, P., Vanhoorelbeke, K., Mannik, A., and Voorberg, J. (2019) Modifying ADAMTS13 to modulate binding of pathogenic autoantibodies of patients with acquired thrombotic thrombocytopenic purpura. *Haematologica.***105**(11):2619-2630.
8. Gao, W., Anderson, P. J., and Sadler, J. E. (2008) Extensive contacts between ADAMTS13 exosites and von Willebrand factor domain A2 contribute to substrate specificity. *Blood*. **112**, 1713–1719
9. Muia, J., Zhu, J., Gupta, G., Haberichter, S. L., Friedman, K. D., Feys, H. B., Deforche, L., Vanhoorelbeke, K., Westfield, L. A., Roth, R., Tolia, N. H., Heuser, J. E., and Sadler, J. E. (2014) Allosteric activation of ADAMTS13 by von Willebrand factor. *Proc. Natl. Acad. Sci. U. S. A.* **111**, 18584–9
10. South, K., Freitas, M. O., and Lane, D. A. (2017) A Model for the Conformational Activation of the Structurally Quiescent Metalloprotease ADAMTS13 by Von Willebrand Factor. *J. Biol. Chem.* **292**, 5760–5769
11. Porter, S., Clark, I. M., Kevorkian, L., and Edwards, D. R. (2005) The ADAMTS metalloproteinases. *Biochem. J.* **386**, 15–27
12. Gaboriaud, C., Gregory-Pauron, L., Teillet, F., Thielens, N. M., Bally, I., and Arlaud, G. J. (2011) Structure and properties of the Ca2+-binding CUB domain, a widespread ligand-recognition unit involved in major biological functions. *Biochem. J.* **439**, 185–193
13. Blanc, G., Font, B., Eichenberger, D., Moreau, C., Ricard-Blum, S., Hulmes, D. J. S., and Moali, C. (2007) Insights into how CUB domains can exert specific functions while sharing a common fold: Conserved and specific features of the CUB1 domain contribute to the molecular basis of procollagen C-proteinase enhancer-1 activity. *J. Biol. Chem.* **282**, 16924–16933

14. Greenspan, D. S. (2005) Biosynthetic processing of collagen molecules. *Top. Curr. Chem.* **247**, 149–183
15. Reigstad, L. J., Varhaug, J. E., and Lillehaug, J. R. (2005) Structural and functional specificities of PDGF-C and PDGF-D, the novel members of the platelet-derived growth factors family. *FEBS J.* **272**, 5723–5741
16. Hooi, C. F., Blancher, C., Qiu, W., Revet, I. M., Williams, L. H., Ciavarella, M. L., Anderson, R. L., Thompson, E. W., Connor, A., Phillips, W. A., and Campbell, I. G. (2006) ST7-mediated suppression of tumorigenicity of prostate cancer cells is characterized by remodeling of the extracellular matrix. *Oncogene*. **25**, 3924–3933
17. Milner, C. M., and Day, A. J. (2003) TSG-6: A multifunctional protein associated with inflammation. *J. Cell Sci.* **116**, 1863–1873
18. Major, B., Kardos, J., Kekesi, K. A., Lorincz, Z., Zavodszky, P., and Gal, P. (2010) Calcium-dependent conformational flexibility of a CUB domain controls activation of the complement serine protease C1r. *J. Biol. Chem.* **285**, 11863–11869
19. Birn, H., Verroust, P. J., Nexø, E., Hager, H., Jacobsen, C., Christensen, E. I., and Moestrup, S. K. (1997) Characterization of an epithelial ~460-kDa protein that facilitates endocytosis of intrinsic factor-vitamin B12 and binds receptor-associated protein. *J. Biol. Chem.* **272**, 26497–26504
20. Zheng, X., Chung, D., Takayama, T. K., Majerus, E. M., Sadler, J. E., and Fujikawa, K. (2001) Structure of von Willebrand Factor-cleaving Protease (ADAMTS13), a Metalloprotease Involved in Thrombotic Thrombocytopenic Purpura. *J. Biol. Chem.* **276**, 41059–41063
21. Zhou, Z., Yeh, H. C., Jing, H., Wang, C., Tao, Z., Choi, H., Aboulfatova, K., Li, R., and Dong, J. F. (2011) Cysteine residues in CUB-1 domain are critical for ADAMTS13 secretion and stability. *Thromb. Haemost.* **105**, 21–30
22. Yeh, H. C., Zhou, Z., Choi, H., Tekeoglu, S., May, W., Wang, C., Turner, N., Scheiflinger, F., Moake, J. L., and Dong, J. F. (2010) Disulfide bond reduction of von Willebrand factor by ADAMTS-13. *J. Thromb. Haemost.* **8**, 2778–2788
23. Bao, J., Xiao, J., Mao, Y., and Zheng, X. L. (2014) Carboxyl terminus of ADAMTS13 directly inhibits platelet aggregation and ultra large von willebrand factor string formation under flow in a free-thiol-dependent manner. *Arterioscler. Thromb. Vasc. Biol.* **34**, 397–407
24. Rottensteiner, H., Seyfried, B. K., Kaufmann, S., Fiedler, C., Dong, J. F., Zheng, X. L., Plaimauer, B., and Scheiflinger, F. (2019) Identification of cysteine thiol-based linkages in ADAMTS13 in support of a non-proteolytic regulation of von Willebrand factor. *J. Thromb. Haemost.* **17**, 2099–2109
25. Muia, J., Zhu, J., Greco, S. C., Vanhoorelbeke, K., Gupta, G., Westfield, L. A., and Evan Sadler, J. (2019) Phylogenetic and functional analysis of ADAMTS13 identifies highly conserved domains essential for allosteric regulation. *Blood.* **133**, 1899–1908
26. Zanardelli, S., Chion, A. C. K., Groot, E., Lenting, P. J., Mckinnon, T. a. J., Laffan, M. a., Tseng, M., and Lane, D. a. (2009) A novel binding site for ADAMTS13 constitutively exposed on the surface of globular VWF. *Thromb. Haemost.* **114**, 2819–2828
27. Pos, W., Crawley, J. T. B., Fijnheer, R., Voorberg, J., Lane, D. A., and Luken, B. M. (2010) An autoantibody epitope comprising residues R660, Y661, and Y665 in the ADAMTS13 spacer domain identifies a binding site for the A2 domain of VWF. *Blood*. **115**, 1640–1649

28. Jin, S.-Y., Skipwith, C. G., and Zheng, X. L. (2010) Amino acid residues Arg659, Arg660, and Tyr661 in the spacer domain of ADAMTS13 are critical for cleavage of von Willebrand factor. *Blood*. **115**, 2300–2310
29. Crawley, J. T. B., De Groot, R., Xiang, Y., Luken, B. M., and Lane, D. A. (2011) Unraveling the scissile bond: How ADAMTS13 recognizes and cleaves von Willebrand factor. *Blood*. **118**, 3212–3221
30. Petri, A., Kim, H. J., Xu, Y., de Groot, R., Li, C., Vandenbulcke, A., Vanhoorelbeke, K., Emsley, J., and Crawley, J. T. B. (2019) Crystal structure and substrate-induced activation of ADAMTS13. *Nat. Commun.* **10**, 1–16
31. Schelpe, A., Petri, A., Roose, E., Pareyn, I., Deckmyn, H., Meyer, S. F. De, Crawley, J. T. B., and Vanhoorelbeke, K. (2020) Antibodies that conformationally activate ADAMTS13 allosterically enhance metalloprotease domain function. *Blood Adv.* **4**, 1072–1080
32. Deforche, L., Roose, E., Vandenbulcke, A., Vandeputte, N., Feys, H. B., Springer, T. A., Mi, L. Z., Muia, J., Sadler, J. E., Soejima, K., Rottensteiner, H., Deckmyn, H., De Meyer, S. F., and Vanhoorelbeke, K. (2015) Linker regions and flexibility around the metalloprotease domain account for conformational activation of ADAMTS-13. *J. Thromb. Haemost.* **13**, 2063–2075
33. Yu, S., Liu, W., Fang, J., Shi, X., Wu, J., Fang, Y., and Lin, J. (2019) AFM Imaging Reveals Multiple Conformational States of ADAMTS13. *J. Biol. Eng.* **13**, 1–11
34. Roose, E., Schelpe, A. S., Joly, B. S., Peetermans, M., Verhamme, P., Voorberg, J., Greinacher, A., Deckmyn, H., De Meyer, S. F., Coppo, P., Veyradier, A., and Vanhoorelbeke, K. (2018) An open conformation of ADAMTS-13 is a hallmark of acute acquired thrombotic thrombocytopenic purpura. *J. Thromb. Haemost.* **16**, 378–388
35. Roose, E., Schelpe, A.-S., Tellier, E., Sinkovits, G., Joly, B. S., Dekimpe, C., Kaplanski, G., Le Besnerais, M., Mancini, I., Falter, D. T., von Auer, C., Feys, H. B., Reti, M., Rossmann, H., Vandenbulcke, A., Pareyn, I., Voorberg, J., Greinacher, A., Benhamou, Y., Deckmyn, H., Fijnheer, R. R., Prohaszka, Z., Peyvandi, F., Lämmle, B., Coppo, P., De Meyer, S., Veyradier, A., and Vanhoorelbeke, K. (2020) Open ADAMTS13, induced by antibodies, is a biomarker for subclinical immune-mediated thrombotic thrombocytopenic purpura. *Blood*. 10.1182/blood.2019004221
36. Krieger, E., Joo, K., Lee, J., Lee, J., Raman, S., Thompson, J., Tyka, M., Baker, D., and Karplus, K. (2009) Improving physical realism, stereochemistry, and side-chain accuracy in homology modeling: Four approaches that performed well in CASP8. *Proteins Struct. Funct. Bioinforma.* **77**, 114–122
37. Van Zundert, G. C. P., Rodrigues, J. P. G. L. M., Trellet, M., Schmitz, C., Kastritis, P. L., Karaca, E., Melquiond, A. S. J., Van Dijk, M., De Vries, S. J., and Bonvin, A. M. J. J. (2016) The HADDOCK2.2 Web Server: User-Friendly Integrative Modeling of Biomolecular Complexes. *J. Mol. Biol.* **428**, 720–725
38. Verbij, F. C., Stokhuijzen, E., Kaijen, P. H. P., Alphen, F. Van, Meijer, A. B., and Voorberg, J. (2016) Identification of glycans on plasma-derived ADAMTS13. *Blood*. **128**, 51–59
39. de Vries, S. J., and Bonvin, A. M. J. J. (2011) Cport: A consensus interface predictor and its performance in prediction-driven docking with HADDOCK. *PLoS One*. **6**, e17695

40. Jian, C., Xiao, J., Gong, L., Skipwith, C. G., Jin, S. Y., Kwaan, H. C., and Zheng, X. L. (2012) Gain-of-function ADAMTS13 variants that are resistant to autoantibodies against ADAMTS13 in patients with acquired thrombotic thrombocytopenic purpura. *Blood*. **119**, 3836–3843
41. Maier, J. A., Martinez, C., Kasavajhala, K., Wickstrom, L., Hauser, K. E., and Simmerling, C. (2015) ff14SB: Improving the Accuracy of Protein Side Chain and Backbone Parameters from ff99SB. *J. Chem. Theory Comput.* **11**, 3696–3713
42. Miller, B. R., McGee, T. D., Swails, J. M., Homeyer, N., Gohlke, H., and Roitberg, A. E. (2012) MMPBSA.py: An efficient program for end-state free energy calculations. *J. Chem. Theory Comput.* **8**, 3314–3321
43. Dekimpe, C., Roose, E., Tersteeg, C., Joly, B. S., Dewaele, A., Horta, S., Pareyn, I., Vandenbulcke, A., Deckmyn, H., Feys, H. B., Tellier, E., Kaplanski, G., Scully, M., Coppo, P., De Meyer, S. F., Veyradier, A., and Vanhoorelbeke, K. (2020) Anti-ADAMTS13 autoantibodies in immune-mediated thrombotic thrombocytopenic purpura do not hamper ELISA-based quantification of ADAMTS13 antigen. *J. Thromb. Haemost.* **18**, 985–990
44. South, K., Luken, B. M., Crawley, J. T. B., Phillips, R., Thomas, M., Collins, R. F., Deforche, L., Vanhoorelbeke, K., and Lane, D. A. (2014) Conformational activation of ADAMTS13. *Proc. Natl. Acad. Sci.* **111**, 18578–18583
45. Roose, E., Veyradier, A., and Vanhoorelbeke, K. (2020) Insights into ADAMTS13 structure: impact on thrombotic thrombocytopenic purpura diagnosis and management. *Curr. Opin. Hematol.* **27**, 320–326
46. Gilardin, L., Delignat, S., Peyron, I., Ing, M., Lone, Y. C., Gangadharan, B., Michard, B., Kherabi, Y., Sharma, M., Pashov, A., Latouche, J. B., Hamieh, M., Toutirais, O., Loiseau, P., Galicier, L., Veyradier, A., Kaveri, S., Maillère, B., Coppo, P., and Lacroix-Desmazes, S. (2017) The ADAMTS131239-1253 peptide is a dominant HLA-DR1-restricted CD4+ T-cell epitope. *Haematologica*. **102**, 1833–1841
47. Verbij, F. C., Turksma, A. W., De Heij, F., Kaijen, P., Lardy, N., Fijnheer, R., Sorvillo, N., Ten Brinke, A., and Voorberg, J. (2016) CD4+ T cells from patients with acquired thrombotic thrombocytopenic purpura recognize CUB2 domain-derived peptides. *Blood*. **127**, 1606–1609
48. Sorvillo, N., Pos, W., Berg, L. M. Van Den, Fijnheer, R., Martinez-pomares, L., Teunis, B., Herczenik, E., and Voorberg, J. (2012) The macrophage mannose receptor promotes uptake of ADAMTS13 by dendritic cells The macrophage mannose receptor promotes uptake of ADAMTS13 by dendritic cells Copyright © 2012 American Society of Hematology. **119**, 3828–3836
49. Sorvillo, N., Van Haren, S. D., Kaijen, P. H., Ten Brinke, A., Fijnheer, R., Meijer, A. B., and Voorberg, J. (2013) Preferential HLA-DRB1*11–dependent presentation of CUB2-derived peptides by ADAMTS13-pulsed dendritic cells. *Blood*. **121**, 3502–3510
50. Hattori, N., Kuwana, M., Kaburaki, J., Mimori, T., Ikeda, Y., and Kawakami, Y. (2000) T cells that are autoreactive to β2-glycoprotein I in patients with antiphospholipid syndrome and healthy individuals. *Arthritis Rheum.* **43**, 65–75
51. Nowak, A. A., O'Brien, H. E. R., Henne, P., Doerr, A., Vanhoorelbeke, K., Laffan, M. A., and McKinnon, T. A. J. (2017) ADAMTS-13 glycans and conformation-dependent activity. *J. Thromb. Haemost.* **15**, 1155–1166

52. Nagae, M., and Yamaguchi, Y. (2012) Function and 3D structure of the N-glycans on glycoproteins. *Int. J. Mol. Sci.* **13**, 8398–8429

53. Obser, T., Id, A. L., Lehmann, K., Mess, C., Ko, G., Peine, S., Schneppenheim, S., Budde, U., Schneider, S. W., Schneppenheim, R., and Id, M. A. B. (2020) ADAMTS13 variants possess proteolytic activity at the surface of endothelial cells and in simulated circulation. *PLoS One*. **15**, 1–18

54. Shang, D., Zheng, X. W., Niiya, M., and Zheng, X. L. (2006) Apical sorting of ADAMTS13 in vascular endothelial cells and Madin-Darby canine kidney cells depends on the CUB domains and their association with lipid rafts. *Blood*. **108**, 2207–2215

Tables and Figures

Table 1: All ADAMTS13 variants and their concentration levels

	ADAMTS13 construct	Concentrated medium	Antigen levels (µg/ml)
CUB1	WT	no	2.8
	D1240A	yes	1.2
	D1240R	yes	0.0
	M1241A	no	3.4
	R1247A	no	2.0
	R1247E	no	2.1
	D1240-41A	yes	1.9
	D1240-41-47A	yes	0.6
	L1243A	no	2.0
	L1248A	no	1.3
	L1243-48A	no	0.9
	D1240-41-43-47-48A (5x-CUB1)	yes	1.6
CUB2	P1333A	no	0.7
	R1336A	no	1.3
	R1336E	yes	1.4
	E1382A	no	1.3
	E1382R	no	1.8
	S1383A	no	2.1
	S1384A	no	2.2
	R1336-83-84A	yes	0.6
	P1333-36-82-83-84A (5x-CUB2)	yes	0.4

Table 2: Overview of proteolytic activity and conformational status of ADAMTS13 CUB domain variants

	ADAMTS13 construct	Activity against FRETS-VWF73 (relative to WT in %)	Activity against VWF multimers (relative to WT in %)	Conformational status
	WT	100	100	Closed
CUB1	D1240A	N/A	>100	Open
CUB1	M1241A	≈100	0	Closed
CUB1	L1243A	≈100	≈100	Closed
CUB1	R1247A	≈100	≈100	Closed
CUB1	R1247E	≈100	≈100	Open
CUB1	D1240-41A	N/A	>100	Open
CUB1	D1240-41-47A	N/A	>100	Open
CUB1	L1243A	≈100	>100	Open
CUB1	L1248A	135	>100	Intermediate
CUB1	L1243-48A	180	>100	Open
CUB1	D1240-41-43-47-48 (5x-CUB1)	N/A	>100	Open
CUB2	P1333A	≈100	>100	Open
CUB2	R1336A	100	100	Closed
CUB2	R1336E	N/A	>100	Open
CUB2	E1382A	≈100	>100	Closed
CUB2	E1382R	≈100	>100	Intermediate
CUB2	S1383A	≈100	≈100	Closed
CUB2	S1384A	≈100	≈100	Closed
CUB2	R1336-83-84A	N/A	>100	Open
CUB2	P1333-36-82-83-84A (5x-CUB2)	N/A	>100	Open

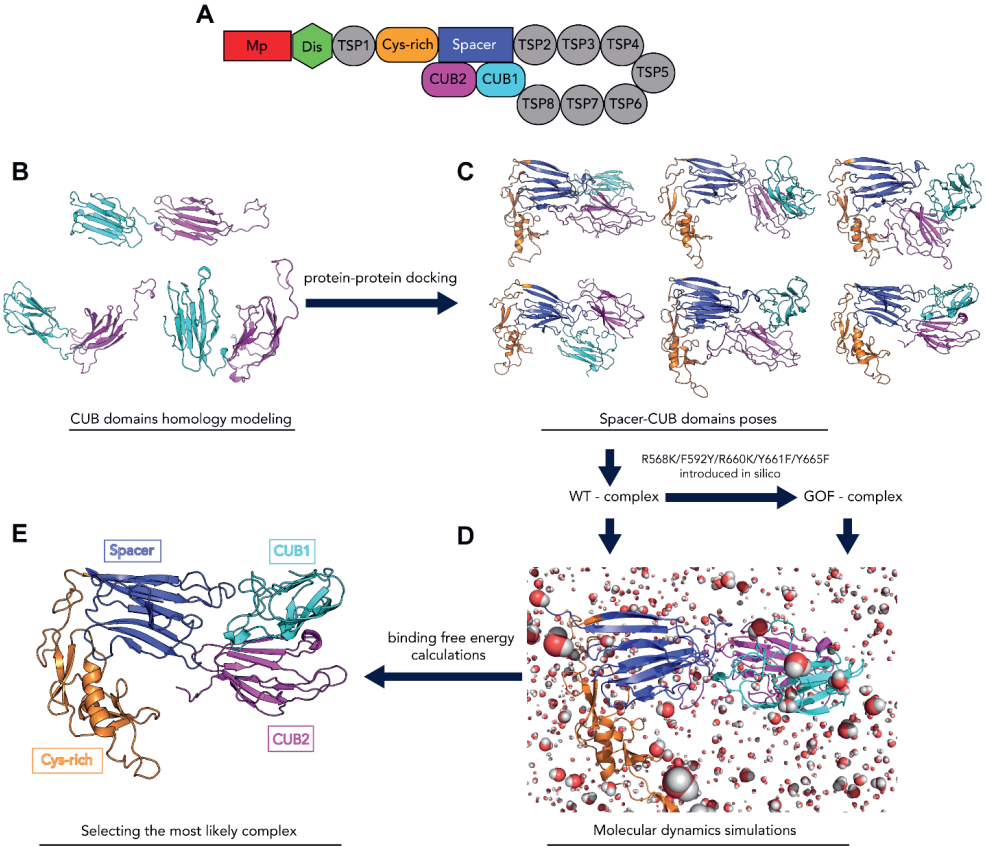

Figure 1 – Building ADAMTS13 closed conformation model.

A. ADAMTS13 closed conformation domain organization. **B.** Homology modeling of ADAMTS13 CUB domains based on three different templates (PDB ID: 4gz9 (top), 2qql (bottom left), 3kq4 (bottom right). **C.** Possible complexes between ADAMTS13 spacer domain and CUB domains after protein-protein docking. **D.** All docking results were duplicated and GoF-ADAMTS13 mutations were introduced to each duplicate. Both WT- and GoF- complexes were introduced to molecular dynamics simulations. **E.** Binding free energy (BFE) calculations were computed each identical WT- and GoF- complex. Our selection criteria on selecting the most likely complex was based on BFE should be much lower for WT-complex (higher affinity) than GoF-complex. Selected most likely complex model was further investigated at a residue level to identify the mediators of closed conformation.

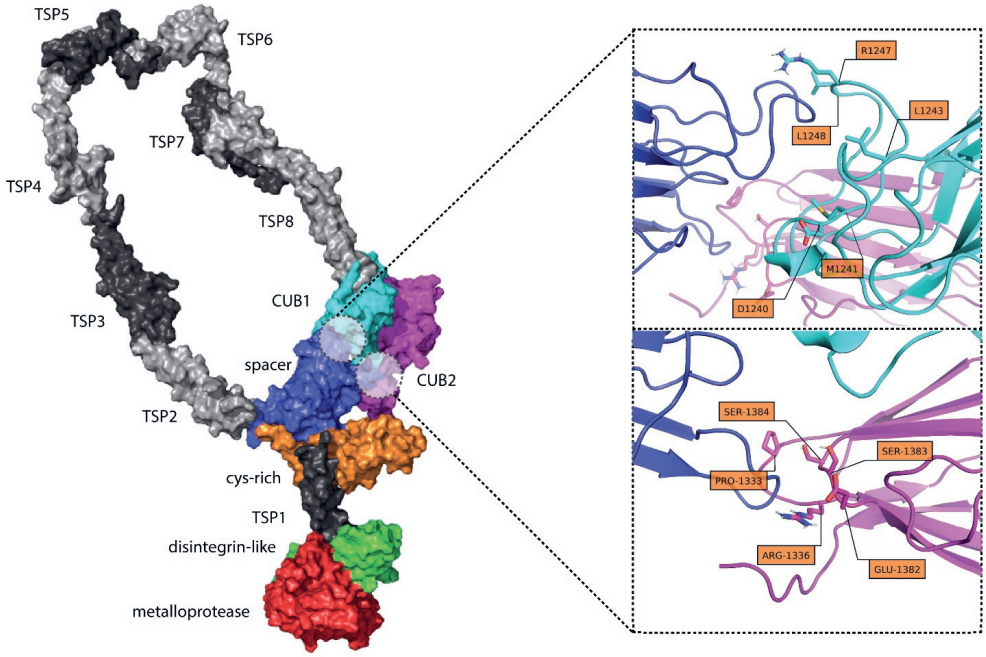

Figure 2 – ADAMTS13 closed conformation 3D model close up.

The Model predicted several residues from both CUB1 and CUB2 domain interacting with spacer domain.

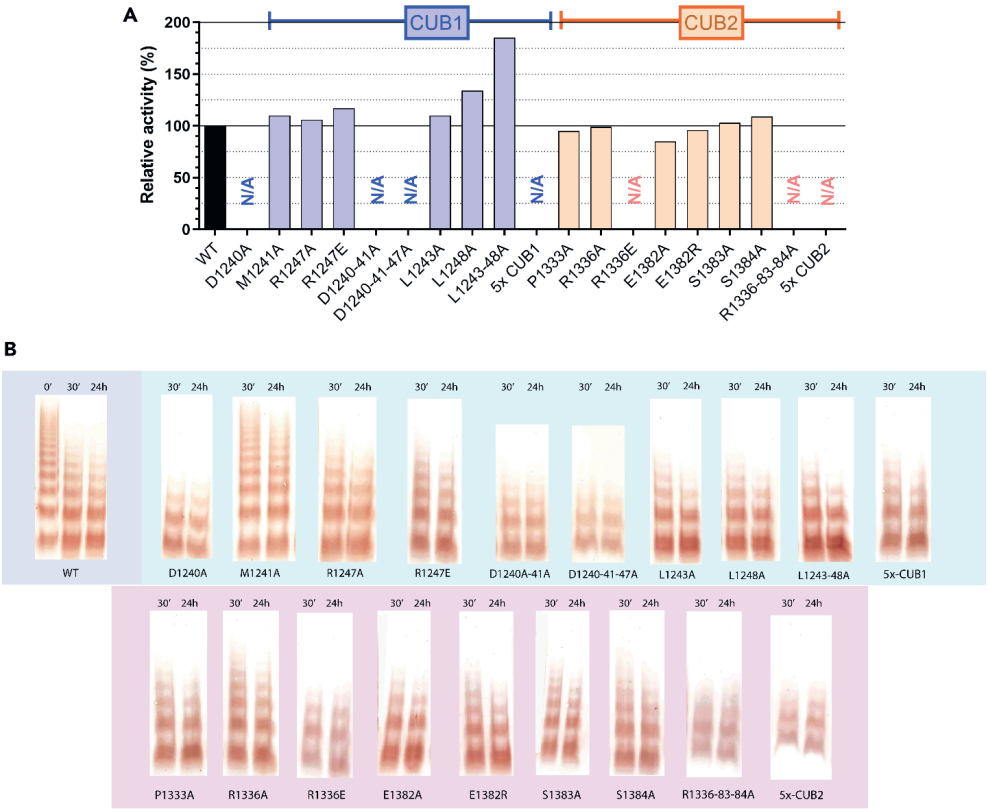

Figure 3 – Proteolytic activities of ADAMTS13 variants.

A. ADAMTS13 variants activity measurement by FRETS-VWF73 assay. All activities were calculated relative to WT-ADAMTS13 (100%). **B.** ADAMTS13 variants activity measurement by VWF multimer assay. VWF cleavage samples were collected at 0 minute, 30 minutes, and 24 hours' time points. N/A (not analyzed).

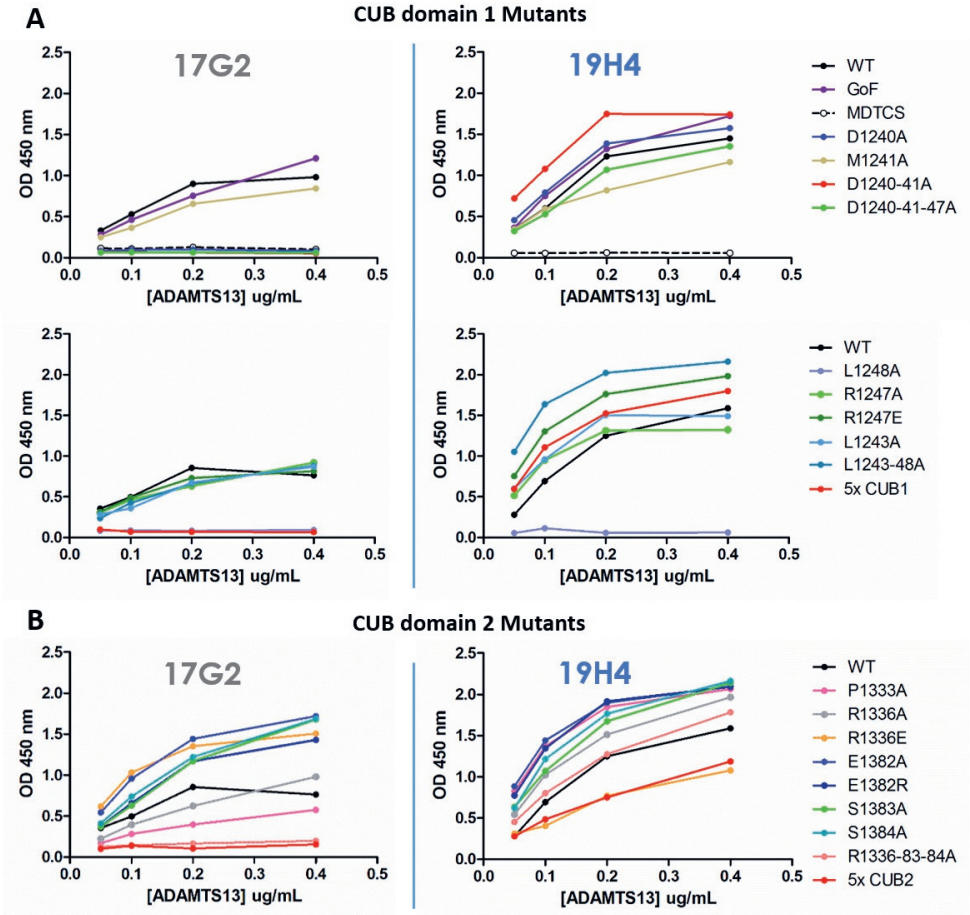

Figure 4 – Dose-response curves of 17G2 (anti-CUB1) and 19H4 (anti-TSP8) binding to WT-ADAMTS13 CUB1 and CUB2 domain variants, and to MDTCS.

A. 17G2 binds to WT-ADAMTS13, but not to MDTCS lacking the C-terminal TSP2-CUB2 domains. The D1240A substitution in the CUB1 domain disrupts the 17G2 epitope in all mutants it is present. All of the other variants are still able to bind to 17G2. Mutant L1248A is an odd exception to both antibodies, since the double mutant L1243-48A clearly bound each. All CUB1 mutants bound to 19H4. **B.** All ADAMTS13 CUB2 variants bound well to both antibodies, except mutants E1382-83-84A and the 5xCUB2.This is likely due to low concentrations of these mutants.

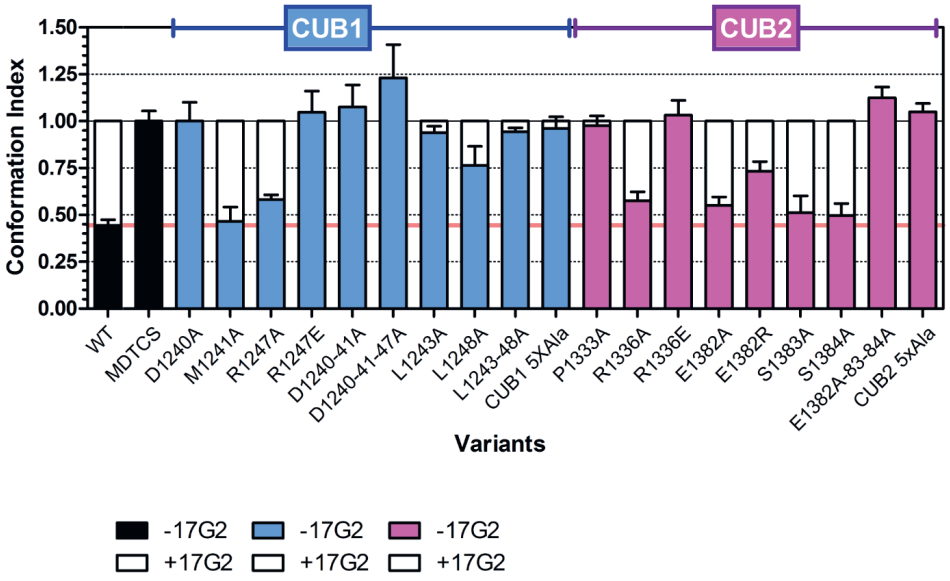

Figure 5 – Open-closed conformation screening of ADAMTS13 CUB domain variants.

Bars in black correspond to WT- and MDTCS-ADAMTS13. Bars in cyan belong to CUB1 domain variants, bars in magenta belong to CUB2 domain variants. A threshold level in red is behind the bars indicate WT-ADAMTS13 conformation as a reference of closed conformation for the CUB domains.